Re-Establishment Of Design Formula For Post-Buckling Shear Strength Of Practical Plate Girder

Thi-Hang Mai*

Department of Civil Engineering, Vietnam Aviation Academy, Viet Nam

***Corresponding Author/ E-mail: hangmt@vaa.edu.vn**

Manuscript received: October 2, 2024 / Revised: November 1, 2024 / Accepted: November 20, 2024

ABSTRACT

A plate web subjected to shear load is well-known for its capability to develop remarkable post-buckling shear strength when two pairs of boundary conditions of the web panel are provided sufficiently. So far, there are some theories and numerous idealizations to explain this behaviour. Still, all of the existing web post-buckling theories need to be revised, and thus, the elusive phenomena during the post-buckling stage remain a great challenge to researchers. By the finite element analysis results combined with the existing experimental shear tests, the previous paper (Mai TH et al, 2017) not only shed light on the weaknesses in the existing theories but also revealed new findings concerning the sources of the web post-buckling reserve. The current paper continuously conducted intensive investigations of the web post-buckling behaviour in the plate I-girders under shear load by a set of models, and the behaviour of intermediate transverse stiffeners was studied simultaneously. Consequently, the current results revealed that the boundary condition behaviour at the junction between transverse stiffeners and web panels depended primarily on the size of web panels (a/D). Next, a new design formula for ultimate shear strength in practical girders was proposed based on the observed results from the set of models. Finally, its accuracy was verified by 48 existing test specimens that possessed slight and moderate flanges.

KEYWORDS: Web buckling, ultimate shear strength, intermediate transverse stiffener, shear post-buckling strength

NOMENCLATURE

X, Y, Z = Coordinate system
k = shear buckling coefficient
Vcr = shear buckling strength
Vp = plastic buckling strength
Vu = ultimate buckling strength
VBP = post-buckling strength
a = transverse stiffener spacing
bf = flange width
D = girder depth
tf , tw = flange, web thickness
E = Young's modulus
□ = Poisson's ratio

1. Introduction

In the previous paper (Mai TH et al, 2017) by Mai et al., the thorough literature review indicated the strengths as well as the weaknesses of the existing theories. In general, the classical theories related to the web post-buckling issue in plate girders were based on analytical and experimental investigations. Although the classical theories and modified classical models differed in the distribution of the tension field and the failure mechanism, all of them were based on the fundamental assumptions that the web post-buckling reserve was contributed primarily by the in-plane tension field in the web panel. Basler (Basler, K. 1961a, 1962b, 1961c) assumed that the tension stress formed in a part of the web panels after the buckling. In this mechanism, the flanges did not participate in the equilibrium of the web panels, but the transverse stiffeners were similar to anchors to be balanced to the tension stress in the post-buckling stage. In the theoretical models, Basler used the separate web panels under shear load, which neglected the frame action as in Figure. 1. However, Basler then used a series of test specimens on the different model which included the frame action to verify the accuracy of his formula as in Figure.2

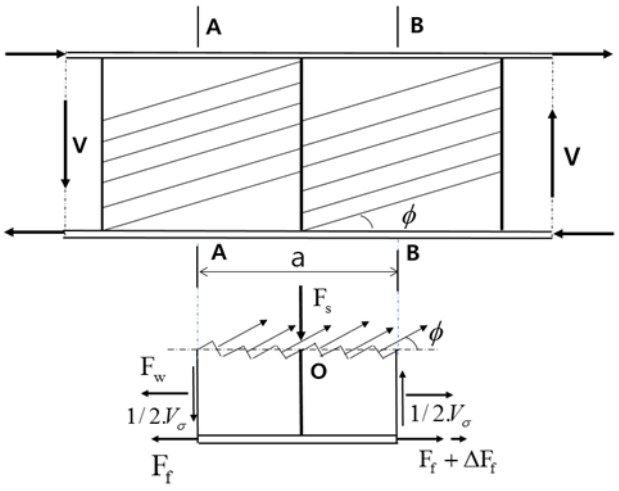

Figure 1: Basler's model in theoretical study.

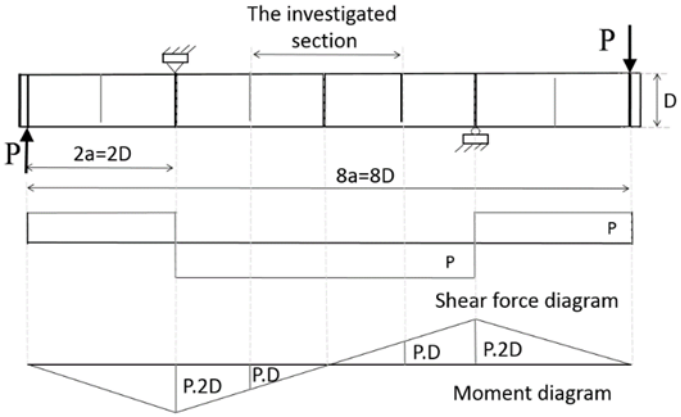

Figure 2: Basler's model in experimental study.

Basler (Basler, K. 1961a, 1962b) supposed that flanges were too flexible to resist the induced force from the tension field. This assumption implied that Basler's theory should be adopted for the girders with from the slight flanges to the moderate flanges. Later on, Fujii (Fujii T, 1968) and Chern and Ostapenko (Chern A, 1969) presented the different tension field which spread through the whole cross-sectional area with the variable intensity as depicted in Figure. 3(b).

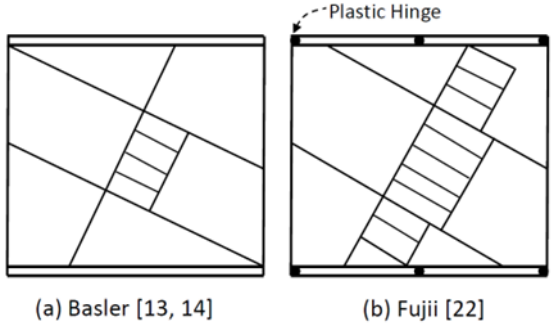

Figure 3: Various tension fields.

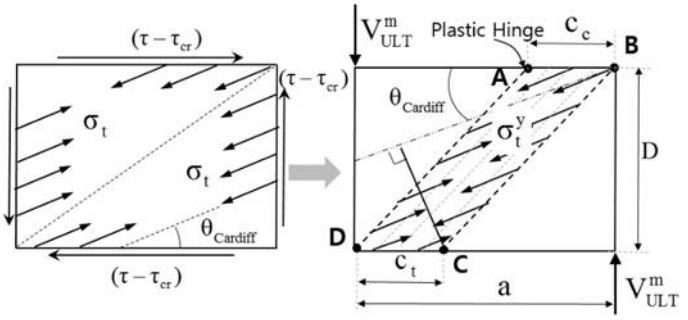

Figure 4: Development of tension field in Porter's model (Cardiff model).

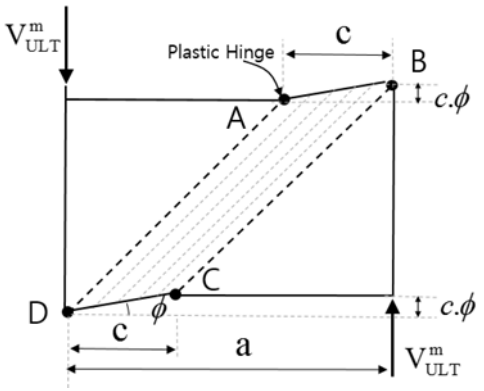

Figure 5: Collapse mechanism of Porter's model (Cardiff model).

Porter et al. (Porter, 1975) introduced a novel collapse mechanism in which the yielding zone ABCD develops when the tensile stress equals the yield stress, as depicted in Figure. 4. Subsequently, the formation of plastic hinges on the flanges leads to the collapse of the girder, as simulated in Figure. 5. This model, later referred to as the Cardiff model, became a foundational reference in the study of girder collapse mechanisms.

Over the past decades, contemporary researchers such as (Lee SC et al, 1998, 1999, 2002, 2003), (Se-Kwon Jung, 2006) and (Donald, 2008), (M.M Alinia, 2009, 2011), and (Mai TH et al, 2017) have critically examined the limitations of classical tension theories. While these theories can reasonably predict ultimate shear strength within certain parameter ranges for plate girders, significant inconsistencies persist, as highlighted by the following points:

1. As assumed in classical tension theories, the equilibrium of web panels during the post-buckling stage remains questionable.
2. Based on in-plane tension, classical post-buckling theories fail to account for the geometrically nonlinear behaviour inherent in the post-buckling stage.

3. The singular model used in classical theories must adequately capture the full range of web post-buckling behaviour across practical girder parameters.
4. Findings in (Mai TH et al, 2017) demonstrated that in-plane tension, posited in classical theories, does not predominantly contribute to the web post-buckling reserve strength

Numerical methods have enabled contemporary researchers to achieve greater clarity in simulating web post-buckling behaviour. For instance, Lee and Yoo (Lee SC et al, 1998) employed an idealized model consisting of a single web panel and flanges, excluding transverse stiffeners and frame action. While this simplification provided the lowest estimate of ultimate shear strength, detailed analyses in (Mai TH et al, 2017) revealed inaccuracies in the boundary conditions assumed in Lee and Yoo's model.

Subsequently, (M.M Alinia, 2009, 2011) conducted investigations using a fixed aspect ratio of 1 and concluded that Basler's formula overestimated girder shear resistance. Studies by Lee and Yoo (Lee SC et al, 1998) and (Mai TH et al, 2017) further demonstrated that Basler's formula and derivatives overestimated shear resistance for girders with an aspect ratio a/D=1. Still, they underestimated it for girders with a/D≥2. This finding highlights the insufficiency of studying girders with a fixed aspect ratio to represent web post-buckling behaviour across all practical scenarios, necessitating further analysis of girders with longer web panels.

White et al. extended this research by investigating full-scale girder models with pre-selected transverse stiffener sizes to ensure sufficient web post-buckling strength development. However, as evaluated in (Mai TH et al, 2017), this finite element (FE) model provided an upper bound for shear resistance. It was deemed unsuitable for practical design formulation, although it offered valuable insights into post-buckling behaviour.

The proliferation of theories addressing web post-buckling behaviour underscores the complexity and inconsistencies inherent in this phenomenon, as no single model has yet provided a comprehensive explanation. As a result, web post-buckling behaviour remains a challenging area of investigation, attracting considerable attention from researchers.

In conventional analyses, transverse stiffeners have received limited focus, typically assumed to meet the requirements for web post-buckling development and modelled with supported boundary conditions. To address this gap, the present study examines the size and behaviour of transverse stiffeners in conjunction with web post-buckling phenomena.

Despite significant progress, understanding the real web post-buckling behaviour under shear forces remains a formidable challenge. This study investigates the post-buckling behaviour of plate I-girders under shear loads using models that specifically incorporate intermediate transverse stiffeners. The authors aim to comprehensively explain web post-buckling behaviour across practical girder parameters and propose a reliable design formula for predicting the ultimate shear strength of steel plate I-girders.

2. Behavior of intermediate transverse stiffeners

The current part considered the requirements of the intermediate transverse stiffeners that can divide the web panel successfully into smaller panels. The web panel with D/tw = 200 was selected, and the expected sub-web panel size was equivalent to a/D=1. With the depth of the girder, D = 2032 mm, the width of the flange was taken about D/3, 610 mm. The thickness ratio of the flange to the web tf/tw was 3. Young's modulus = 210 GPa, the yield stress = 345 MPa and Poisson's ratio = 0.3 were used in the numerical analyses. The analyzed model is presented in Figure. 6.

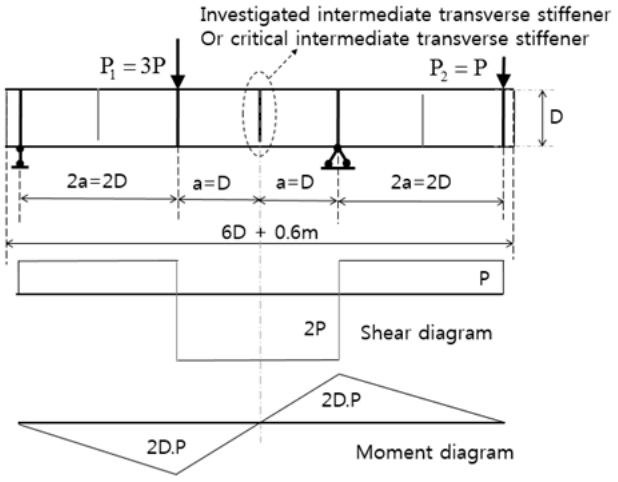

Figure 6: Investigated model for intermediate transverse stiffeners.

The initial sizes of intermediate transverse stiffeners were based upon the required moment of inertia as:

$$I_t \geq a.t_w^3 J \qquad (1)$$

$$J = 2.5(D/a)^2 - 2.0 \geq 0.5$$

The transverse stiffener moment of inertia It was computed about the mid-thickness of the web panel. The transverse stiffener width was limited based on (AASHTO, 1998, 2004, 2012, 2020) as expressed:

$$b_t \leq 0.48 t_p \sqrt{(E / F_{ys})} \qquad (2)$$

Where: bt is the transverse stiffener width; tP is the transverse stiffener thickness; Fys is the yield strength of stiffeners;

Subsequently, the sizes of intermediate transverse stiffeners were increased gradually by increasing their areas first and then by increasing their moment of inertia as shown in summary in Table 1. Additionally, the models had four pairs of 250×30 mm bearing stiffeners at their ends and load points as well

Table 1: Intermediate transverse stiffener sizes

Types	I	II	III	IV	V
Sizes	80x7	80x18	120x12	120x16.3	140x30
A(mm2)	560	1440	1440	1960	4200
I_S/I_{SCR}	1.12	2.88	6.49	8.81	25.75

I_S : Moment inertia of intermediate transverse stiffener;

I_{SCR} : Minimum required moment inertia based Eq. (1)

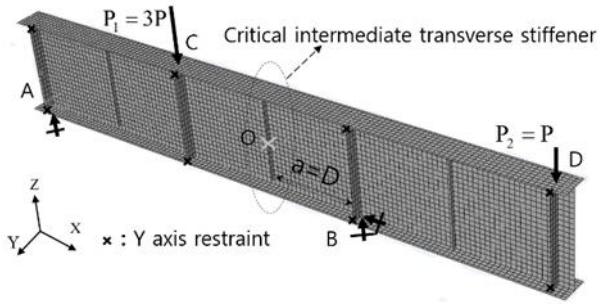

Figure 7: Boundary condition and load used in Abaqus.

The girder model was composed of three spans. It was simply restricted in the Y direction at the top and the bottom of all bearing stiffeners to be against the lateral displacement. The bearing stiffeners were created at supported and loaded positions, and two pairs of bearing stiffeners on the end panels were set up 300mm from the edge of the girder. Intermediate transverse stiffeners were in between the bearing stiffeners. The model was supported vertically at the bottom of the bearing stiffeners at locations A and B, as indicated in Figure. 7. The restraint along the X direction was only modelled at the bottom line cross B. With the forced boundary condition, the concentrated loads were placed on lines across C and D points with the amplitude of P and 3P, respectively. Each force was loaded at three positions to avoid concentrated stress. Three-quarters of a total magnitude was loaded at the web-flange junction, and one-eighth of the force was placed on two sides of this position.

Table 2: FE results for the selected girder

Types	I	II	III	IV	V
Sizes	80x7	80x18	120x12	120x16.3	140x30
V_U (kN)	2422.8	2698.1	2873.9	2874.7	2875.9
W_O (mm)	39.0	20.0	7.3	6.0	3.5

W_O : Maximum deflection of O point

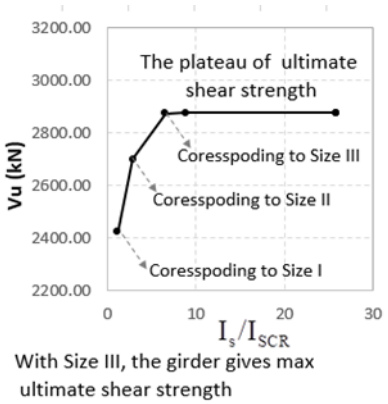

Figure 8: Ultimate shear strength values against various size of intermediate transverse stiffeners.

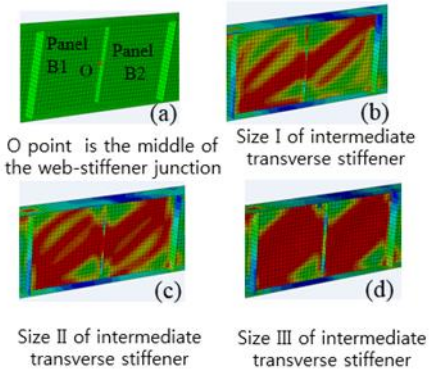

Figure 9: Failure mode of web panel against various size of intermediate transverse stiffeners.

The analyzed results are summarized in Table 2. For intermediate transverse stiffeners with dimensions 80×7 mm, the maximum deflection at the midpoint of the critical stiffeners was 39 mm. In this case, the post-buckling mode of the web panel exhibited an interactive mode spanning two adjacent panels, as illustrated in Figure. 9(b). When the stiffener cross-sectional area increased to 80×18 mm (2.6 times the initial area), the ultimate shear strength improved from 2422.8 kN to 2698.1 kN, and the deflection at point O reduced to 20 mm. The failure mode remained interactive, as shown in Figure. 9(c).

Subsequently, with stiffener dimensions maintained at 120×12 mm but the moment of inertia increased to 6.49 times the initial value, the ultimate shear strength reached 2873.9 kN. Further increases in stiffener sizes, such as 120×16.3 mm and 140×30 mm, did not result in additional increases in ultimate shear strength, as shown in Figure. 8. However, deflection at point O continued to decrease, as reflected in the fourth row of Table 2. These findings suggest that the maximum ultimate shear strength was achieved at a stiffener size of 120×12 mm.

These observations show that intermediate transverse stiffeners primarily function as bending rather than compressive components. To effectively divide the web panel into sub-panels as intended, the intermediate transverse stiffener must satisfy a minimum required moment of inertia.

Furthermore, from observation in Figure. 8, the ultimate shear strength of investigated girders increased gradually with the increase in Is. However, the ultimate shear strength rose slowly against the extra growth in the size of the transverse stiffener when Is approached a certain value. Then, the ultimate shear strength was maintained at the plateau range regardless of an extra increase in the stiffener size. It is concluded that the value at the plateau of ultimate shear strength was the maximum ultimate shear strength in the investigated girder and was a manifestation of the successful subdivision of the web panel. The required intermediate transverse stiffener has yet to be determined in the present research. Therefore, the following part used the plateau of ultimate shear strength to gain the girders' maximum ultimate shear strength.

It is also noticeable that some prior researchers, such as Lee and Yoo (Lee SC et al, 2002), believed that the maximum ultimate shear strength was a manifestation to express the full developing potential post-buckling in a girder. However, as in the above discussion, the maximum ultimate shear strength indicated that the web panel was successfully divided into two smaller panels by the minimum required intermediate transverse stiffener. It is also emphasized that the web panel worked in an interactive post-buckling mode before ultimate shear strength approached the maximum value.

3. Set of the current models

This study used two models: the full-scale girder model with various sizes of intermediate transverse stiffeners and the single isolated panel model with zero rigidity of transverse stiffener. With each set of investigated parameters (slenderness ratio, aspect ratio), the full-scale girder model aimed to provide girders' maximum ultimate shear strength. The single isolated panel model was expected to give the minimum ultimate shear strength of girders.

3.1. The full-scale girder model

First, as in Figure.10, the full-scale girder model was used to obtain the girders' maximum ultimate shear strength. This model included the full contribution of the flange and the transverse stiffeners. The dimensions were: D = 2032mm (80 in), bf = 610 mm (about D/3), tf/tw = 3. The main variables were the slenderness ratio, D/tw and the aspect ratio, a/D. The sizes of the intermediate transverse stiffeners were also variables. Corresponding to each main variable of the girder, the sizes of the intermediate transverse stiffeners varied until the maximum ultimate shear strength of girders was obtained through the plateau range. Besides, the model had four pairs of bearing stiffeners with the size of 250 x 3. tf at supported points and loaded points. Two pairs of outside bearing stiffeners were 300mm from the edge of the girders. This model type was named Model No1 (a) and was described in Figure. 11.

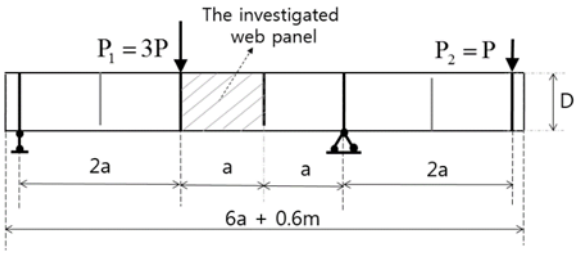

Figure 10: Full-scale girder model.

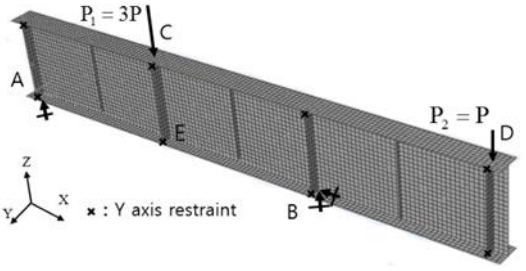

Figure 11: Load and boundary condition in Model No1 (a) in Abaqus.

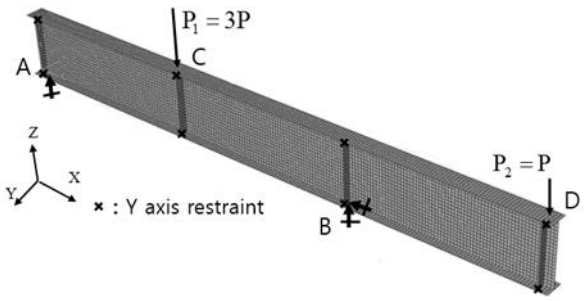

Figure 12: Load and boundary condition in Model No1 (b) in Abaqus**.**

The initial intermediate transverse stiffener sizes were chosen based on Eq. (1) and (2). Their values for the moment of inertia rose gradually until all ultimate shear strength values reached the plateau range and gained the maximum ultimate shear strength values. The intermediate transverse stiffener sizes were summarized in Tables 3 and 4. The additional model, Model No1 (b), was quite similar to Model No1 (a) but excluded the intermediate transverse stiffeners. This model was to study the behaviour of long web panels, a/D =3 As in Figure. 12. The boundary conditions and the applied shear were described in Part 2. The initial geometric imperfection was introduced into the full nonlinear analyses based on the first buckling mode shape. The magnitude of the geometrical imperfection was taken within typical fabrication tolerances, 1% of the web thickness.

Table 3: Intermediate transverse stiffeners sizes with aspect ratio =1

Aspect ratio =1	Slenderness ratio					
	90	120	150	200	250	300
Model No1(a)-size 1	140 x 13	120 x 9	100 x 9	80 x 7	70x6	60 x 5
Model No1(a)-size 2	220 x 20	180 x 16	160 x 12	120 x 12	100x 10	90 x 8
Model No1(a)-size 3	220 x 20	180 x 16	160 x 12	120 x 12	140x 14	140x 14
Model No1(a)-size 4	220x 25	180x 20	160x 16	120x 16.3	140x 20	140x 16

Size 1 of intermediate transverse stiffener possessed minimum requited moment inertia;

Table 4: Intermediate transverse stiffeners sizes with aspect ratio=2

Aspect ratio =2	Slenderness ratio					
	90	120	150	200	250	300
Model No1(a)-size 1	170x15	140x11	120x10	90x9	80x7	60x6
Model No1(a)-size 2	260x25	210x20	180x16	140x14	120x 11	120x 12
Model No1(a)-size 3	260x30	210x30	180x20	140x20	120x 15	110x 15

Size 1 of intermediate transverse stiffener possessed minimum requited moment inertia;

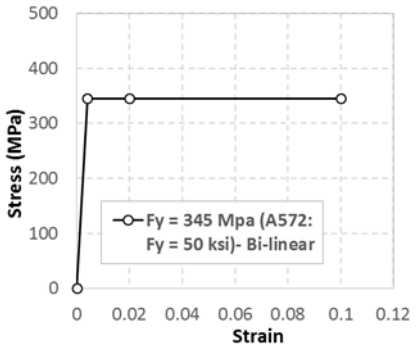

Figure 13: Strain-stress diagram.

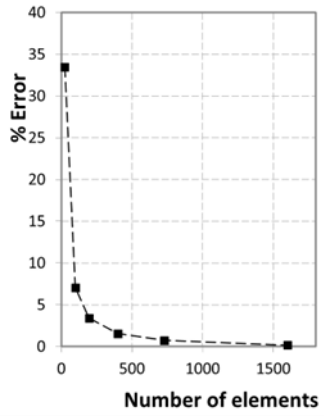

Figure 14: Convergence results from the FE analyses.

All models were conducted in two steps by using Abaqus software. In the first step, the buckle procedure of the linear perturbation option was selected to analyze the Eigenvalue. Then, the first buckling mode shape obtained from the previous step was used to create the initial geometrical imperfection in the studied model. In the second step, the modified Riks method investigated the post-buckling analyses. The S4R shells from the available element library in Abaqus were utilized in both the linear and nonlinear analyses. In this research, A572 steel was used for all components of the studied models with the stress-strain real curve depicted in Figure. 13. Some extra investigations indicated that the Bilinear or Multilinear behaviour of the stress-strain relation did not influence the value of ultimate shear strength. Therefore, the bilinear stress-strain curve was used for these analyses.

In FE analyses, a mesh size was selected reasonably to produce accurate results and reduce the analysis time on Abaqus. Figure.14 presents the convergence results from the studies by the simply supported panel model. For the element size of 0.1x0.1m (the web panel included 400 shell elements), the difference between the buckling shear strength obtained from the FE analysis and the exact solution was only 1.5%. Thus, this mesh refinement type was used for the full nonlinear analyses. The flanges were divided similarly. The yield stress was 345 MPa. Poisson's ratio and elastic modulus were shown in the notation table.

3.2. The single isolated panel model

Herein, the investigated web panel was isolated from the girder to become the single isolated panel model. This ideal model was so-called as Model No2 which was analyzed with all studied parameters as in part 3.1. In general, it was supposed that transverse stiffeners were stiff enough to support the development of the web post-buckling within the separate sub-web panel. For Model No2 as shown in Figure. 15, the two edges at the transverse stiffeners were presumed to be simple supports. The boundary conditions in the modeling procedure, which would be sure the pure shear state in the studied model, were listed in Table 5. The shear force was applied in the form of the uniform shell edge load along the middle surface of plates. The flanges were modeled as the beam elements and the concentrated forces V were assigned at the middle point of the flanges as in Figure.15. This type of models was expected to provide the most conservative prediction for ultimate shear strength in girders.

Herein, the investigated web panel was isolated from the girder to become the single isolated panel model. This ideal model was called Model No2, which was analyzed with all studied parameters as in part 3.1. In general, it was supposed that transverse stiffeners were stiff enough to support the development of the web post-buckling within the separate sub-web panel. For Model No2, as shown in Figure. 15, the two edges at the transverse stiffeners were presumed to be simple supports. The boundary conditions in the modelling procedure, which would ensure the pure shear state in the studied model, are listed in Table 5. The shear force was applied in the form of a uniform shell edge load along the middle surface of the plates. The flanges were modelled as the beam elements, and the concentrated forces V were assigned at the middle point of the flanges, as in Figure.15. This model was expected to provide the most conservative prediction for ultimate shear strength in girders.

Table 5: Boundary condition in Model No2

BC	U_x	U_y	U_z	θ_x	θ_y	θ_z
Edge 1	1	0	0	0	0	0
Edge 2	1	0	0	0	0	0
Edge 3, 4, 7, 8	1	0	0	0	0	0
Edge 5, 6, 9, 10	0	0	0	0	0	0
Point 11	0	1	1	0	0	0
Point 12, 13, 14	0	0	1	0	0	0

1: Restraint ; 0: Free

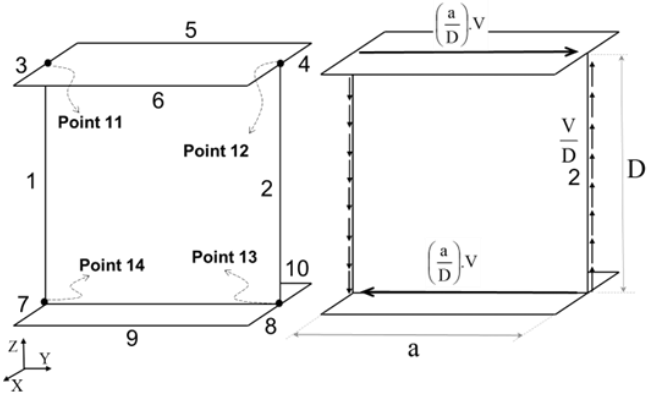

Figure 15: Applied load and boundary condition in Model No2.

4. FEA results and discussion

4.1. The shear buckling coefficient

In this part, the results obtained by using the present models (Model No1 (a), Model No1 (b), Model No2) were compared with the shear buckling strength values calculated by the current design practices AASHTO LRFD [16], Eq. (3) and by Lee and Yoo's Eq. (6).

Shear buckling strength based on [16].

$$V_{cr} = CV_p \tag{3}$$

Herein, C is the ratio of elastic shear strength to plastic shear strength. It was determined based on Eq. (4).

$$\begin{aligned}
&\text{if}: \ \frac{D}{t_w} < 1.12\sqrt{\frac{Ek_{Vincent}}{F_w}} \Rightarrow C = 1.0 \\
&\text{if}: 1.12\sqrt{\frac{Ek_{Vincent}}{F_w}} < \frac{D}{t_w} < 1.4\sqrt{\frac{Ek_{Vincent}}{F_w}} \\
&\Rightarrow C = \frac{1.12}{(D/t_w)}\sqrt{\frac{Ek_{Vincent}}{F_w}} \\
&\text{if}: \ 1.4\sqrt{\frac{Ek_{Vincent}}{F_w}} < \frac{D}{t_w} \\
&\Rightarrow C = \frac{1.57}{(D/t_w)^2}.\left(\frac{Ek_{Vincent}}{F_w}\right)
\end{aligned} \tag{4}$$

$$k_{Vincent} = 5 + \frac{5}{(a/D)^2} \tag{5}$$

Shear buckling strength proposed by Lee et al. (Lee SC et al, 1996).

$$V_{cr} = k_{Lee}.\frac{\pi^2 E}{12(1-\eta^2)(D/t_w)^2} Dt_w \tag{6}$$

With,

$$\begin{aligned}
&k_{Lee} = k_{ss} + \frac{4}{5}(k_{fs} - k_{ss})\left[1 - \frac{2}{3}(2 - \frac{t_f}{t_w})\right] \quad \text{for } \frac{1}{2} \le \frac{t_f}{t_W} < 2 \\
&k_{Lee} = k_{ss} + \frac{4}{5}(k_{fs} - k_{ss}) \qquad \text{for } \frac{t_f}{t_W} \ge 2
\end{aligned} \tag{7}$$

k_{ss} is the shear buckling coefficient when all edges of web panel are simple supports.

$$\begin{aligned}
k_{ss} &= 4.00 + \frac{5.34}{(a/D)^2} \ \text{for} \ a/D < 1 \\
k_{ss} &= 5.34 + \frac{4.00}{(a/D)^2} \ \text{for} \ a/D \ge 1
\end{aligned} \tag{8}$$

k_{sf} is the shear buckling coefficient when two opposite edges of the web panel were simple supports and fixed supports, respectively. And it was computed by Eq. (9).

$$\begin{aligned}
k_{sf} &= \frac{5.34}{(a/D)^2} + \frac{2.31}{a/D} - 3.44 + 8.39(a/D) \ \text{for} \ a/D < 1 \\
k_{sf} &= 8.89 + \frac{5.61}{(a/D)^2} - \frac{1.99}{(a/D)^3} \ \text{for} \ a/D \ge 1
\end{aligned} \tag{9}$$

The comparisons of shear buckling strength obtained from the present analyses and the various equations were presented in Tables 6 and 7. Due to the similarity, the results of web panels with a/D=2 were omitted for brevity.

Table 6. Shear buckling strength for aspect ratio (a/D) = 1

Aspect ratio	1				
Slenderness ratio	90	120	150	200	300
(1) FEM by Model No1 (a)	9035.0	5520.3	2818.52	1207.98	361.69
(2) FEM by Model No2	9134.4	5392.8	2759.4	1180.9	355.7
(1)/(2)	0.99	1.02	1.02	1.02	1.02
(3) Lee&Yoo's E.q (6)	12844.4	5418.7	2787.3	1169.2	346.8
(1)/(3)	0.70	1.02	1.01	1.03	1.04
(4)AASHTO [16]	8753.9	4423.8	2265.0	955.5	283.1
(1)/(4)	1.03	1.25	1.24	1.26	1.28

Table 7: Shear buckling strength for aspect ratio (a/D) = 3

Aspect ratio	3				
Slenderness ratio	90	120	150	200	300
(1) FEM by Model No1 (b)	8242.1	3963.8	2025.7	864.9	258.6
(2) FEM by Model No2	8231.4	4190.0	2141.6	914.6	274.5
(1)/(2)	1.00	0.95	0.95	0.95	0.94
(3) Lee&Yoo's E.q (6)	9429.7	3978.2	2036.8	859.3	254.6
(1)/(3)	0.87	1.00	0.99	1.01	1.02
(4)AASHTO [16]	6017.2	2538.5	1299.7	548.3	162.5
(1)/(4)	1.37	1.56	1.56	1.58	1.59

With a/D=1, the shear buckling strength values obtained from Model No1 (a) were similar to those obtained by Model No2, as illustrated by the ratio (1)/(2) in Table 6. Through the ratio (1)/(3) in the range of slender sections in Table 6, we can see that the predictions of elastic buckling strength by both Model No1(a) and Model No2 were in good agreement with those calculated by Lee and Yoo's Eq. (6) . This behaviour revealed that the flange-web junctions behaved like fixed supports in the elastic analysis regardless of the boundary conditions at transverse stiffeners.

In contrast, for the long web with a/D=3, Model No1 (b) gave the elastic shear buckling strength values, about 95% of the results obtained from Model No2, as presented in the fifth row of Table. 7. It means that there was a reduction in elastic buckling strength in Model No1 (b), which could be due to the free torsion of the flanges as in Figure. 16. However, the smallest values of elastic buckling strength from both models correlated well with Lee and Yoo's predictions.

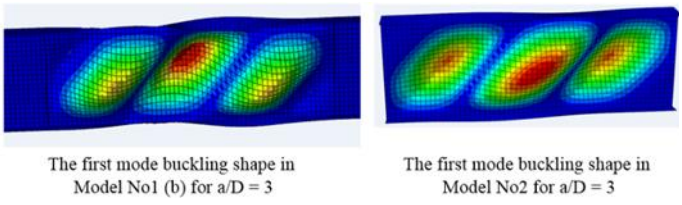

Figure 16: First buckling mode shape in different models.

Besides, Tables 6 and 7 show that the elastic shear buckling values based on AASHTO LRFD (2014) (AASHTO, 2020) were much less than those obtained from Model No1 (a) (or Model No2). It can be concluded that the boundary conditions at the web-flange junctures, which were assumed to be simple supports, were excessively conservative. Particularly, for the plates with a/D=3, the FEM predictions were 60% more than those calculated by (AASHTO, 2020).

Noticeably, all buckling analyses by Lee and Yoo in (Lee SC et al, 1996) were carried out using the linear procedure in MSC/NASTRAN, and because of this, Lee and Yoo's predictions based on Eq. (6) overestimated the inelastic shear buckling of web panels with D/tw <120 as observed in Table 6 and 7.

In brief, the elastic shear buckling strength values obtained from the present finite element analyses in all cases agreed with those calculated by Lee and Yoo's shear buckling coefficient (Lee SC et al, 1996). Therefore, Lee and Yoo's shear buckling coefficient was used reasonably in this research for slender sections.

4.2. Ultimate shear strength

4.2.1. Web panels with aspect ratio =1

The aspect ratio of 1 was discussed at first. The numerical results are presented in Table 8. Columns 2 to 5 show the results obtained from Model No1 (a), in which the sizes of intermediate transverse stiffeners were varied to reach the maximum value of ultimate shear strength. Column 6 includes the results of the single isolated panel model, Model No2.

As illustrated in Figure. 17, with the stiffener size 3, for all web panels in the range of the investigated slenderness ratio, ultimate shear strength values approached the plateau. Thus, it was believed that with size 3 of intermediate transverse stiffeners, the girders provided the maximum ultimate shear strength values, and sub-web panels were divided successfully.

Table 8: Ultimate shear strength (kN) with aspect ratio a/D =1

Aspect ratio = 1					
D/t *w*	Model No1(a) Size 1	Model No1(a) Size 2	Model No1(a) Size 3	Model No1(a) Size 4	Model No2
1	2	3	4	5	6
90	9033.7	9035.0	9035.0	9054.4	9134.4
120	5863.6	5879.8	5879.8	5890.5	5534.0
150	3959.4	4211.9	4211.9	4233.4	3644.3
200	2427.8	2878.3	2878.3	2874.7	2186.0
250	1695.0	1973.1	2146.7	2137.1	1446.6
300	1263.0	1437.2	1700.1	1697.0	1051.3

Model No1(a) includes transverse stiffeners; Size 1, Size 2, Size 3, Size 4 are sizes of intermediate transverse stiffeners

Model No1(a) with Size 3 of intermediate transverse stiffener provides the maximum ultimate shear strength

Model No2: This is ideal model without transverse stiffeners

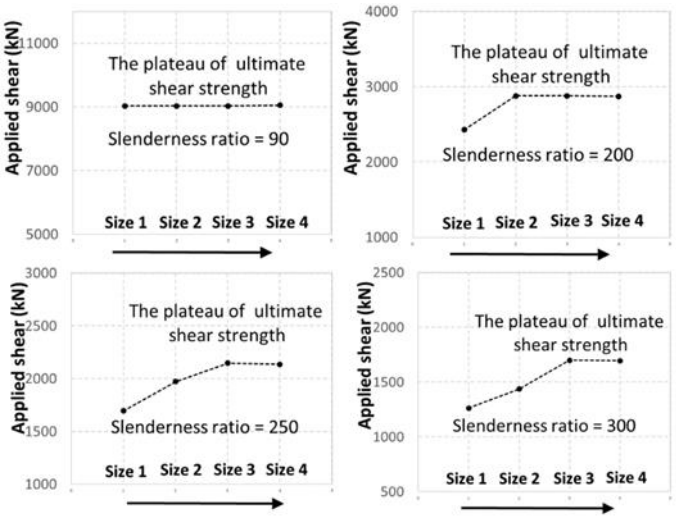

Figure 17: Illustration of the plateau of applied shear against the moment inertia of intermediate transverse stiffeners with a/D =1.

The numerical results from all model types plotted in Figure. 18 show that Model No2 provided the lowest predictions, as shown by line 1. With Model No1 (a), the ultimate shear strength values rose proportionally to the moment inertia of intermediate transverse stiffeners when the sizes of the intermediate transverse stiffeners were not sufficient to approach the plateau, as illustrated by lines 2 and 3. Model No1 (a) provided the highest predictions corresponding to the girders that possessed the stiffener size 3, as illustrated by line 4.

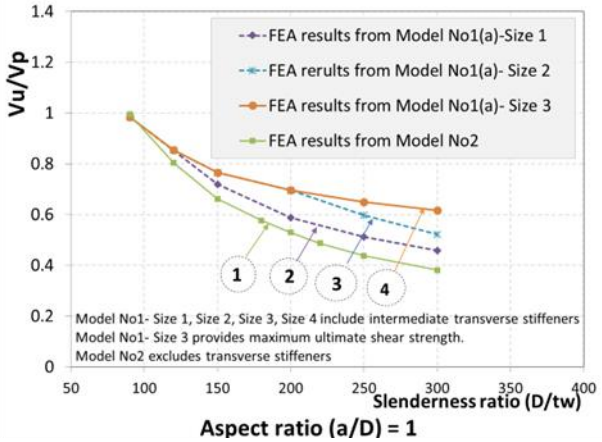

Figure 18: Ultimate shear strength from FEM with various model and various size of intermediate transverse stiffeners.

Table 9: Difference between maximum post-buckling values and minimum post-buckling values (a/D=1)

Aspect ratio = 1					
D/t_w	120	150	200	250	300
V_P	6885.1	5508.1	4131.1	3304.9	2754.1
V_{cr}	5392.8	2759.4	1180.9	603.3	355.7
$V_{U\text{-}min}$	5534.0	3644.3	2186.0	1446.6	1051.3
$V_{U\text{-}max}$	5879.8	4211.9	2878.3	2146.7	1700.1
$V_{BP\text{-}min}/(V_P - V_{cr})\%$	9.5	32.2	34.1	31.2	29.0
$V_{BP\text{-}max}/(V_P - V_{cr})\%$	32.6	52.8	57.5	57.1	56.1
$(V_{BP\text{-}max} - V_{BP\text{-}min})/(V_P - V_{cr})\%$	-	20.6	23.4	25.9	27.1

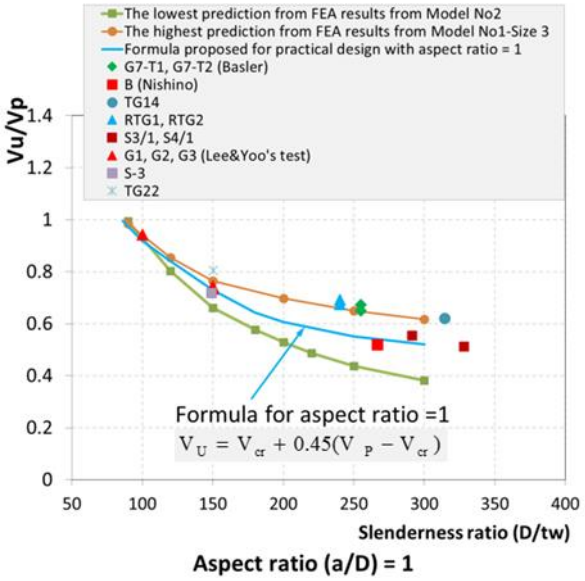

Figure 19: Illustration of the representative curve for a/D = 1.

For the lowest predictions VU-min, it realizes that post-buckling strength, VBP-min was over 32.2% of the difference between VP and Vcr for the slender section. For the low slenderness range, the value of VBP-min was very small compared to Vcr, as calculated in Table 9. However, for the highest predictions VU-max, the post-buckling strength, VBP-max was over 52.8% of the difference between Vp and Vcr .

As shown above, the lowest predictions were obtained from Model No2, in which the rigidity of the

transverse stiffener was equal to zero. In contrast, the highest predictions were determined by Model No1 (a) with the minimum required intermediate transverse stiffeners at least. From observation in Figure. 19, the prediction domain was formed by combining the lowest predictions and the highest predictions. This prediction domain revealed that the rigidity of the required intermediate transverse stiffeners contributed significantly to ultimate shear strength values, over 20.6% of (VP – Vcr), as calculated in Table 9. Consequently, the curve between the lowest bound and the highest bound, VU = Vcr + 0.45(VP – Vcr), was proposed to calculate ultimate shear strength values with the aspect ratio of 1, as described in Figure. 19.

Figure. 19 indicated that the proposed curve was under the test results for all web panels. Therefore, it was expected that the proposed curve could give conservative predictions for practical design.

4.2.2. Web panel with aspect ratio greater than 1

Similarly, the minimum required moment of inertia of intermediate transverse stiffeners based on Eq. (1) and (2) in Model No1 (a) was used initially for web panels with a/D=2. The intermediate transverse stiffener sizes gradually increased until the maximum ultimate shear strength was obtained. This implied that the web panels were divided successfully. The results are given in Table 10 and Figure. 20, Model No1 (a) provided the maximum ultimate shear strength values corresponding to the girders that possessed the stiffener size 2.

Table 10: Ultimate shear strength (kN) with aspect ratio a/D =2

Aspect ratio = 2				
D/tw	Model No1(a) Size 1	Model No1(a) Size 2	Model No1(a) Size 3	Model-No2
1	2	3	4	5
90	8282.5	8284.2	8273.5	8982.5
120	5032.7	5051.5	5019.5	5134.4
150	3481.2	3508.1	3510.1	3348.8
200	2143.8	2270.5	2270.8	1974.1
250	1454.8	1613.0	1615.1	1304.4
300	1085.3	1187.4	1192.6	946.8

Model No1(a) includes transverse stiffeners; Size 1, Size 2, Size 3 are sizes of intermediate transverse stiffeners

Model No1(a) with Size 2 of intermediate transverse stiffener provides maximum ultimate shear strength

Model-No2: is ideal model without transverse stiffeners

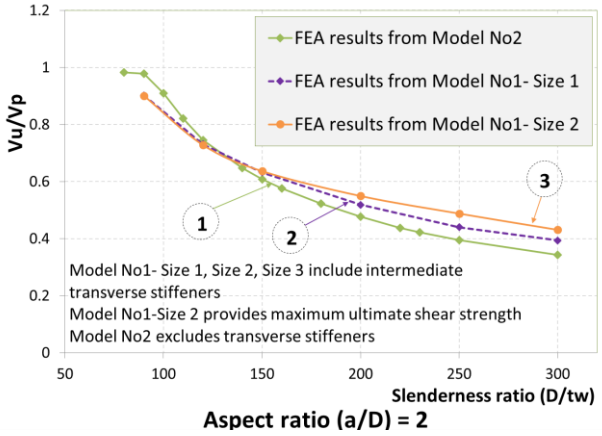

Figure 20: Ultimate shear strength from FEM with various model and various intermediate transverse stiffener sizes (For aspect ratio = 2).

Table 11: Difference between maximum post-buckling values and minimum post-buckling values (a/D=2)

Aspect ratio = 2					
D/t_w	120	150	200	250	300
$(V_{BP\text{-}max} - V_{BP\text{-}min})/(V_P - V_{cr})$%	-4.9	4.9	9.4	11.0	9.8

Figure. 20 shows that the rigidity of the required intermediate transverse stiffeners also contributed to the post-buckling development of long web panels with D/tw≥ 120. The maximum ultimate shear strengths obtained from Model No1-Size 2 were greater than those from Model No2 in the range of the slender section, as shown in Figure. 20. Otherwise, in inelastic ranges, Model No1 (a) provided smaller predictions than those obtained from Model No2, as illustrated by the part of line 3 that is below line 1 in Figure. 20. The reason is that the failure of Model No1 (a) in inelastic sections was caused by the shear and moment mode, which resulted in the reduction in ultimate shear strength.

The comparisons in Table 11 show that the differences between the highest predictions and the lowest predictions of ultimate shear strength values were from 4.9% to 11% of (VP – Vcr); these differences were not significant. Therefore, for long web panels with a/D=2, the lowest bounds were suggested to estimate ultimate shear strength values as shown by the representative curve in Figure. 21. The comparison in Figure. 21 indicated that the representative curve was under the test results for all web panels with a/D=2. Therefore, it was expected that the formula based on the representative curve could give conservative predictions for web panels with a/D =2

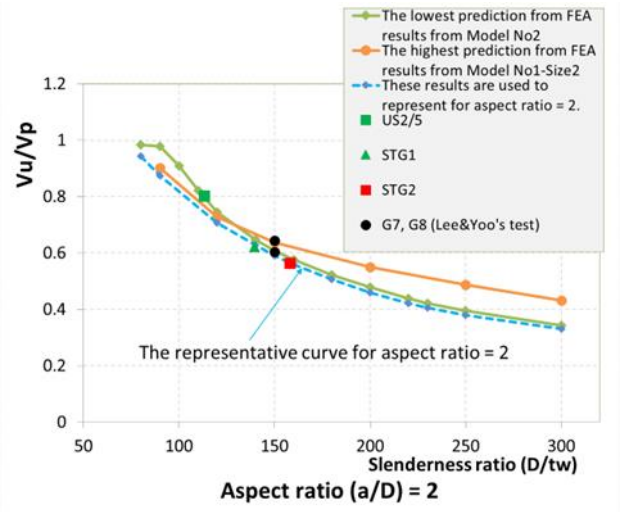

Figure 21: Illustration of the representative curve for a/D = 2.

For panels with a/D=3, Figure. 22 expresses the results of Model No1 (b), which only included bearing stiffeners and Model No2 without transverse stiffeners. It can be found that the bearing stiffeners also contributed to the web post-buckling reserve of girders. However, the maximum difference between the highest and lowest bounds of ultimate shear strengths was only 8.3% of (VP – Vcr), as calculations shown in Table 12. Thus, the lowest bounds, in this case, were also suggested to predict the ultimate shear strengths of girders and illustrated by the representative curve as plotted in Figure. 23. To be similar to the behaviour of web panels with aspect ratio = 2, the representative curve was lower than the test results for all specimens with the aspect ratio = 3 as in Figure. 23. Therefore, it was expected that the formula based on the representative curve could give conservative predictions for a/D =3.

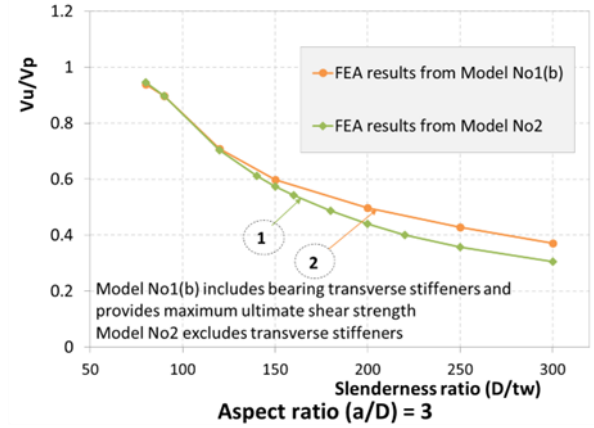

Figure 22: Ultimate shear strength from FEM with various model for a/D = 3.

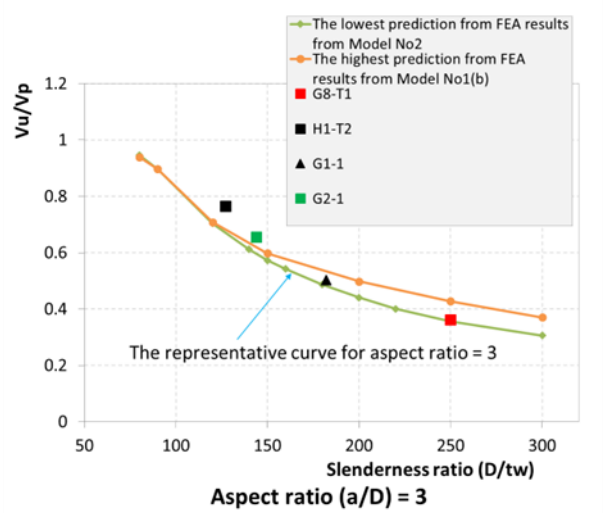

Figure 23: Illustration of the representative curve for a/D = 3.

Table 12: Difference between maximum post-buckling values and minimum post-buckling values (a/D=3)

Aspect ratio = 3					
D/t_w	120	150	200	250	300
V_P	6885.1	5508.1	4131.1	3304.9	2754.1
V_{cr}	4190.0	2141.6	914.6	464.1	274.5
$V_{U\text{-}min}$	4848.0	3156.6	1821.1	1179.4	843.2
$V_{U\text{-}max}$	4879.7	3296.0	2057.5	1414.0	1020.9
$V_{BP\text{-}min}/(V_P - V_{cr})\%$	24.4	30.1	28.2	25.2	22.9
$V_{BP\text{-}max}/(V_P - V_{cr})\%$	25.6	34.3	35.5	33.4	30.1
$(V_{BP\text{-}max} - V_{BP\text{-}min})/(V_P - V_{cr})\%$	1.2	4.1	7.3	8.3	7.2

4.2.3. Proposed design formula for ultimate shear strength

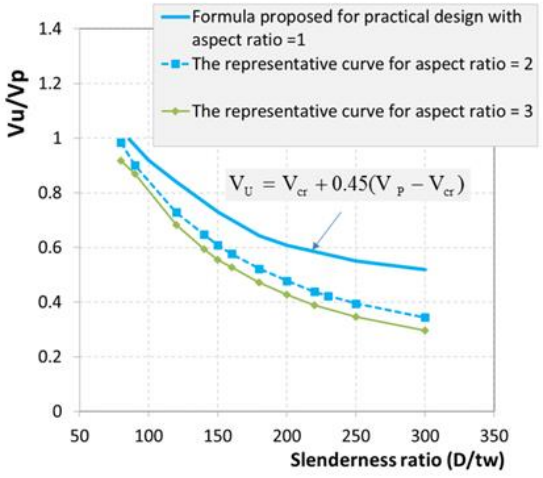

Figure 24: Representative curves for sizes of the web panel.

As in the discussion from the previous part, when the aspect ratio (a/D) =1, post-buckling shear strength V_{BP} was suggested 45% of the difference between plastic post-buckling shear strength and buckling shear strength (VP – Vcr), or VBP = 0.45(VP – Vcr). For the long web panels, the lowest bounds obtained from the FE analyses were suggested for the predictions of ultimate shear strength. As a result, for all investigated parameters, we had the representative curves of sizes of web panels as plotted in Fig 24. To generalize for all ranges of the practical girders, the current study conducted the regression analyses from the representative curves in Figure. 24. Then, the formula for post-buckling shear strength was suggested by the following equation:

$$V_{BP} = \frac{0.45(1-C)}{1+0.25(\frac{a}{D}-1)\sqrt{\frac{a}{D}}} V_P \quad (10)$$

The factor expressed in Eq. (11) is the function of reduction in ultimate shear strength because of the rising of the aspect ratio.

$$\frac{1}{1+0.25(\frac{a}{D}-1)\sqrt{\frac{a}{D}}} \quad \text{With a/D>1} \quad (11)$$

Ultimate shear strength included V_{BP} and V_{Cr} as the following expression

$$V_U = V_{cr} + V_{BP} = \left[C + \frac{0.45(1-C)}{1+0.25(\frac{a}{D}-1)\sqrt{\frac{a}{D}}} \right] V_P$$

(12)

With C is the ratio of elastic shear buckling strength to plastic shear strength $(\tau_{cr}/\tau_y \text{ or } V_{cr}/V_y)$, it can be determined as the following formula.

$$\text{if}: \ \frac{D}{t_w} < \sqrt{\frac{Ek_{Lee}}{F_w}} \Rightarrow C = 1.0$$

$$\text{if}: \ \sqrt{\frac{Ek_{Lee}}{F_w}} \le \frac{D}{t_w} \le 1.4\sqrt{\frac{Ek_{Lee}}{F_w}} \Rightarrow C = \frac{1}{\frac{D}{t_w}}\sqrt{\frac{Ek_{Lee}}{F_w}}$$

$$\text{if}: \ 1.4\sqrt{\frac{Ek_{:Lee}}{F_w}} < \frac{D}{t_w} \Rightarrow C = \frac{1.57}{\left(\frac{D}{t_w}\right)^2}.\left(\frac{Ek_{Lee}}{F_w}\right)$$

(13)

k_{Lee} was presented in Eq. (7), (8) and (9).

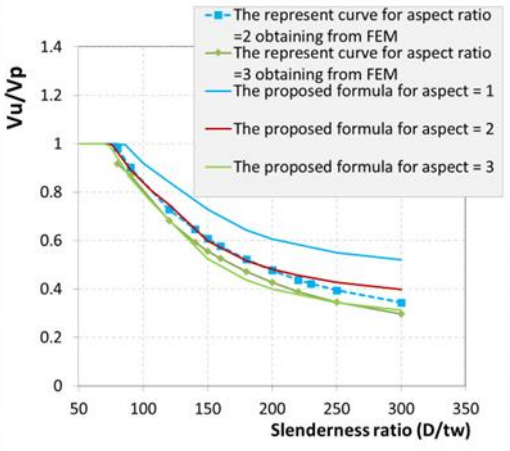

Figure 25: Examination of correlation between representative curves and curves by proposed formula.

The compact section limit in the present research agreed with that in AASHTO. However, when this limit was calculated using the shear buckling coefficient k_{Lee}, some factors needed to be modified as Equation. (13), compared to the original Equation (4) in AASHTO.

For the plastic range of parameters of girders, there was obvious evidence from experimental tests showing that the ultimate shear strength values could be greater than the plastic shear strength values due to the strain-hardening phenomenon. However, the ultimate shear strength values obtained from the experiment not only depended on the yield strength but were also affected by the characteristics of the stress-strain curve. Thus, in general, the plastic shear strength values of the web cross-sections were suggested for plastic ultimate shear strength. The strain-hardening behaviour should be considered in the specific steel grade studies. Figure. 25 shows the good correlation between the representative curves and the curves by the proposed formula. We verified the proposed formula using the existing test results in the following section.

4.2.4. Verification by existing test results

The accuracy of the proposed formula was evaluated by the predictions of ultimate shear strength by different existing models and by the presently proposed formula against a set of 48 experimental test results (Lyse et al, 1935), (Evans, 1984), (Evans, 1986), (Kamtekar et al, 1974), (Rockey et al, 1972), (Adorisio, 1982), (Der Avanessian, 1983), (Sakai F, 1966), (Cooper et al, 1964), (Narayanan, 1981), (Evans et al, 1983), (Kamtekar, 1972), (Bergfelt et al, 1968), (Carskaddan, 1968), (Basler, 1960) and (Nishino, 1968). The considered test specimens had the ratio of the flange to the web (tf/tw) ≤ 4 and the aspect ratio a/D $\leq$ 5.5. The parameters of experimental works were presented in Table 13 in eight groups according to the aspect ratio and the slenderness ratio.

Table 13 indicated that with the aspect ratio of 1, Basler's formula gave greater predictions than test results. When a/D= 1.5, test results correlated well with Basler's prediction. However, for the specimens with a/D $\geq$ 2. Basler's formula underestimated ultimate shear strength, as plotted in Figure. 26.

As discussed in (Mai TH et al, 2017), the suggestion of the strength reduction factor Rd < 1 in (Lee SC et al, 1998) needed to be revised. Because of this reason, Lee and Yoo's equation, including Rd = 1, was utilized to compare with experimental works. Figure. 27 recognizes that Lee and Yoo's model provided acceptable predictions for certain ranges of practical parameters. However, their model provides unsafe predictions for the web panels with a/D $\geq$ 2

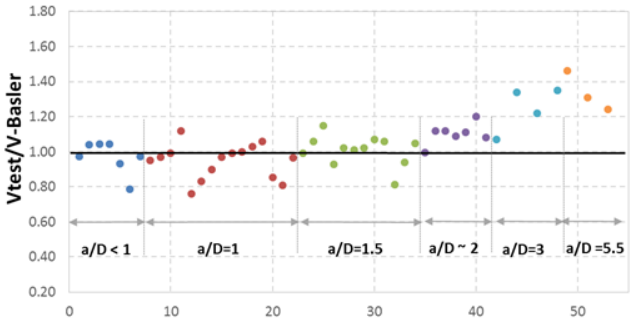

Figure 26: Basler's predictions compared with experimental results

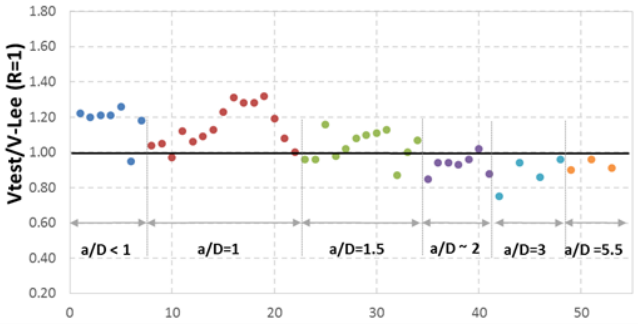

Figure 27: Lee&Yoo's predictions compared with experimental results (By using Lee&Yoo's Eq. in 1998 that includes the reduction factor Rd=1)

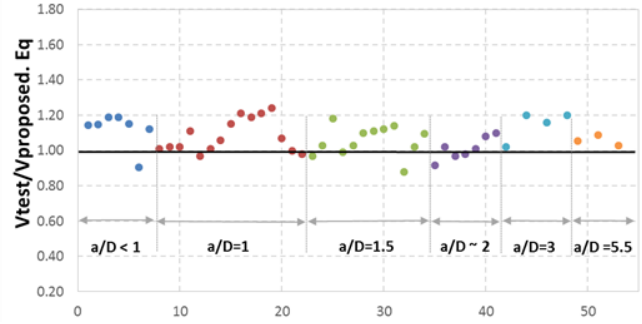

Figure 28: Comparison of predictions by the presently proposed formula with experimental results

Surprisingly, the predictions calculated by the presently proposed formula correlated excellently with test results according to the conservative tendency on all practical parameters, as shown in Figure. 28.

It can be easily recognized that for the web panels with a/D=1, the prediction domain in this research indicated that the contribution of the transverse stiffeners to ultimate shear strength was significant. However, with the rise of the aspect ratio (a/D), the rigidity of the transverse stiffeners decreased its effect on ultimate shear strength. Particularly, with a/D=3, the web-transverse stiffener junctures behaved nearly as simply supported boundary conditions irrespective of the transverse stiffener sizes. This observation revealed that the real behaviour of boundary conditions at transverse stiffener edges disagreed with the

expected behaviour from Lee and Yoo's studied model (Lee & Yoo, 1998).

5. Concluding remarks.

The present research reflected the comprehensive views concerning the post-buckling behaviour of plate webs in practical I-girders, which were summarized in the following conclusions:

1. The intermediate transverse stiffeners needed to meet the minimum required moment inertia value to divide the web panel into the smaller sub-panel in which post-buckling development took place within the single sub-web panel. Meanwhile, in the girders with insufficient intermediate transverse stiffeners, the web panel worked in an interactive post-buckling mode developed in the two adjacent sub-web panels.
2. The observed prediction domain revealed that for a square panel (a/D =1), the rigidity of the required intermediate transverse stiffeners and the bearing stiffeners contributed significantly to ultimate shear strength. However, for long webs a/D ≥ 2, the rigidity of transverse stiffeners reduced its effect on the development of the web post-buckling regardless of stiffener sizes. Even if for a/D= 3, the web-transverse stiffener junctions behaved nearly as simple supports.
3. Both Lee and Yoo's predictions and Basler's predictions were not accurate on the whole range of practical parameters. All existing models themselves included inconsistencies stemming from each theory's misleading assumptions.
4. The currently proposed formula gave reliable predictions for ultimate shear strength in all practical parameters with the aspect ratio (a/D) ≤ 5.5 and the slight and moderate flanges tf/tw ≤ 4.

In current works, the key finding was that the behaviour of the web-transverse stiffener junctions varied according to the web panel aspect ratio. Therefore, the extent of contribution by the flanges, the transverse stiffeners and the frame action to the shear resistance may depend on the size of the web panels.

Shortly, work will be presented on the real web post-buckling mechanism under shear load, and each component of the contribution to the ultimate shear strength will be clarified.

References

Mai TH, Han SY, Kim DH, Kang YJ (2017). The evaluation of the previous models used to study the web post-buckling. International Journal of Steel Structures. International Journal of Steel Structures, 17(3), 1131-1143, 2017.

Basler, K. (1961a). New provisions for plate girder design. Proc., AISC Nat. Engrg. Conf., 65–74.

Basler, K. (1961b). Strength of plate girders under combined bending and shear. J. Struct. Div., ASCE, 87(7), 181–197.

Basler, K. (1963). Strength of plate girders in shear. Trans. ASCE, Vol. 128, Part 11, 683–719.

Fujii T. (1968). On an improved theory for Dr. Basler's theory. Final Rep., IABSE 8th Congress, New York.

Chern C,Ostapenko A. (1969). Ultimate strength of plate girders under shear. Fritz Engineering laboratory report No. 328.7. Lehigh university USA.

Porter DM, Rockey KC, Evans HR. (1975). The collapse behavior of plate girders loaded in shear. Struct Eng 1975;53(8):313–25.

Lee SC, Yoo CH (1998). Strength of plate girder web panels under pure shear. Journal of Structural Engineering, ASCE; 24(2):184–94.

Lee SC, Yoo CH (1999). Experimental study on ultimate shear strength of web panels. Journal of Structural Engineering, ASCE; 125(8):838– 46.

Lee SC, Yoo CH (2002). Behavior of intermediate transverse stiffeners attached on web panels. Journal of Structural Engineering, ASCE; 125(8):838– 46.

Lee SC, Yoo CH (2003). New design rule for intermedia transverse stiffeners attached on web panels. Journal of Structural Engineering, ASCE; 129:1607-1614.

Se-Kwon Jung, Donald W. White. (2006). Shear strength of horizontally curved steel I-girders-finite element analysis studies. Journal of Constructional Steel Research 62 (2006) 329–342.

Donald W. White, Michael G. Barker. (2008). Shear Resistance of Transversely Stiffened Steel I-Girders. J. Struct. Eng. 2008.134:1425-1436.

M.M. Alinia, Maryam Shakiba, H.R. Habashi. (2009). Shear failure characteristics of steel plate girders. Thin-Walled Structures 47 (2009) 1498–1506

M.M. Alinia, Maryam Shakiba, H.R. Habashi. (2011). Postbuckling and ultimate state of stresses in steel plate girders. Thin-Walled Structures 49 (2011) 455–464

AASHTO. (2020). American Association of State Highway and Transportation Officials. (2020). AASHTO LRFD Bridge Design Specifications, 9th Edition. Washington, D.C.: AASHTO.

AASHTO (2012). Guide specifications for horizontally curved steel girder highway bridges with design examples for I-girder and box-girder bridges. Washington (DC): American Association of State and Highway Transportation Officials;

AASHTO (2004). Guide specifications for horizontally curved steel girder highway bridges with design examples for I-girder and box-girder bridges. Washington (DC): American Association of State and Highway Transportation Officials;

AASHTO (1998). Guide specifications for horizontally curved steel girder highway bridges with design examples for I-girder and box-girder bridges. Washington (DC): American Association of State and Highway Transportation Officials;

Lee SC, Davidson JS, Yoo CH (1996) Shear buckling coefficients of plate girder web panels. Computers & Structures 1996;59(5):789–95.

Lyse, I. and Godfrey, H. J. (1935). Investigation of web buckling in steel beams. Transactions A.S.C.E, Paper No, 1907, p. 675, 1935.

Evans H. R. (1984). A Report on the Full Scale Tests in a Girder with a Stiffened Web Subjected to Combined Shear and Bending Loads. University of Wales College of Cardiff, 1984, report DT/SC/12, Nov.

Evans H. R. (1986). An appraisal, by full scale testing, of new design procedures for steel girders subjected to shear and bending. Proceedings of the Institution of Civil Engineers, Part 2, 1986, 81, 175-189.

Kamtekar A. G., Dwight J. B. and Threlfall B. D. (1974). Tests on Hybrid Plate Girders (Report 3). Cambridge University, Cambridge, 1974, Report No. CUED/V-Struct/TR41.

Rockey K. C. and Skaloud M. (1972). The ultimate load behavior of plate girders loaded in shear. The structural Engineer, 1972, 50, No1. 1, 29-48.

Adorisio D. (1982). Model studies on Plate girders Subject to Shear Loading. MSc thesis, University of Wales College of Cardiff, 1982.

Der Avanessian N. G. V. (1983). Ultimate strength of Plate Girders Containing Opening in Webs. PhD thesis, University of Wales College of Cardiff, 1983.

Sakai F, Fujii T. and Fukuchi Y. (1966). Failure Tests of Plate Girders Using Large-sided Models. University

Nishino, F., and Okumura, T. (1968). “Experimental investigation of strength of plate girders in shears.” Proc., 8th Cong. Of the Int. Assoc. of Bridge and Struct. Engrg., New York, N.Y.

of Tokyo, Department of Civil Engineering, Tokyo, 1966, structural Engineering Report.

Cooper P. B., Lew H.S. and Yen B. T. (1964). Welded constructional alloy steel plate girders. Proceedings of ASCE, Structural Division, 1964, 90, No. ST1, 1-36.

Narayanan R. and Rockey K. C. (1981). Ultimate load capacity of plate girders with webs containing circular cut-outs. Proceedings of the Institution of Civil Engineers. Part 2, 1981, 71, 845-862.

Evans H. R. and Tang K.H. (1983). An Investigation of the Ultimate Load Behavior of Longitudinally Stiffened Plate Girder Webs Load Behavior of Longitudinally Stiffened Plate Girder Webs Loaded Predominantly in Shear. University of Wales College of Cardiff, 1983, Report DT/SC/11, Mar.

Kamtekar A. G., Dwight J. B. and Threlfall B. D. (1972). Tests on Hybrid Plate Girders (Report 2). Cambridge University, Cambridge, 1972, Report No. CUED/C-Struct/TR28.

Bergfelt A. and Hovik J. (1968). Thin-walled deep plate girders under static loads. Proceedings of the LABSE colloquium, New York, 1968.

Carskaddan P. S. (1968). Shear buckling of unstiffened hybrid beams. Proceedings of ASCE, Structural Division, 1968, 94, No. ST8, 1965-1990

Basler K., Yen B.T. (1960). Web buckling tests on welded plate girders. Welding Research Council, New York, 1960, Bullentin No. 64. Sept.

.

Table 13. Compared the test results with predictions by various formulas

Girder Test	Ref	D	a/D	D/t_w	t_w	t_f/t_w	E	f_{yw}	V_{test}	V_{test}/V_{Basler}	V_{test}/V_{Lee} $R_d<$	V_{test}/V_{Lee} $R_d=1$	$V_{test}/V_{propose}$
G6-T3	Basler [35]	127	0.5	259.2	4.9	4.04	21000	253	787	0.97	1.22	1.22	1.14
MCS1-	Evans H. R [22]	100	0.7	227.1	4.4	3.43	21000	169.7	388	1.04	1.34	1.20	1.15
PB3	Evans H. R [23]	100	0.7	227.3	4.4	3.43	20500	169.7	388	1.04	1.35	1.21	1.19
PB4	Evans H. R [23]	100	0.7	227.3	4.4	3.43	20500	169.7	388	1.04	1.35	1.21	1.19
G6-T2	Basler [35]	127	0.7	259.2	4.9	4.04	21000	253	662	0.93	1.26	1.26	1.15
TS1/3	Kamtekar.A.G.	813	0.8	200.2	4.06	2.96	21000	265	312	0.78	1.00	0.95	0.91
TS1/4	Kamtekar.A.G.	813	0.8	200.2	4.06	2.96	21000	265	387	0.97	1.24	1.18	1.12
Mean										0.97	1.25	1.18	1.12
G2	Lee [9]	600	1	150	4	2.50	20500	318.5	332.	0.95	1.15	1.04	1.01
G3	Lee [9]	600	1	150	4	3.75	20500	318.5	337.	0.97	1.16	1.05	1.02
G1	Lee [9]	400	1	100	4	3.75	20500	318.5	282.	0.99	1.20	0.97	1.02
TG22	Rockey K. C [25]	305	1	150.3	2.03	3.20	21000	229	79.0	1.12	1.31	1.12	1.11
Mean										1.01	1.21	1.05	1.04
B	Nishino [36]	120	1	266.7	4.5	2.67	21000	490	760	0.76	1.06	1.06	0.97
S4/1	Adorisio D. [26]	351	0.9	328.0	1.07	2.99	20000	169	21	0.83	1.09	1.09	1.01
S3/1	Adorisio D. [26]	300	1	291.3	1.03	3.11	20000	169	19	0.90	1.13	1.13	1.06
G7-T1	Basler [35]	127	1	255.0	4.98	3.92	21000	253	623	0.97	1.23	1.23	1.15
TG14	Rockey K. C [25]	305	1	314.4	0.97	3.22	21000	219	25	0.99	1.31	1.31	1.21
G7-T2	Basler [35]	127	1	255.0	4.98	3.92	21000	253	645	1.00	1.28	1.28	1.19
RTG1	Rockey K. C [25]	305	1	240.2	1.27	3.54	21000	244	40	1.03	1.28	1.28	1.21
RTG2	Rockey K. C [25]	305	1	240.2	1.27	3.70	21000	244	41	1.06	1.32	1.32	1.24
RCP1/	Der Avanessian	718	0.9	357.2	2.01	4.03	21000	271	127	0.85	1.19	1.19	1.07
S5/1	Adorisio D. [26]	399	1	366.1	1.09	2.94	20000	169	23	0.81	1.08	1.08	1.00
S-3	Sakai F. [28]	477	1.2	149.1	3.2	3.28	21000	317	198	0.97	1.09	1.00	0.98
Mean										0.92	1.19	1.18	1.10
G5	Lee [9]	600	1.5	150	4	2.50	20500	318.5	286.	0.99	1.03	0.96	0.97
G4	Lee [9]	400	1.5	100	4	3.75	20500	318.5	268.	1.06	1.17	0.96	1.03
G2-2	Nishino [36]	950	1.5	144	6.6	2.88	21000	486	1225	1.15	1.17	1.16	1.18

Mean										1.07	1.12	1.03	1.06
S3/1.5	Adorisio D. [26]	301	1.5	292.2	1.03	3.11	20000	169	16	0.93	0.98	0.98	0.99
S2/1.5	Adorisio D. [26]	249	1.5	237.1	1.05	3.05	20000	169	16	1.02	1.02	1.02	1.03
G1-2	Nishino [36]	120	1.5	182.0	6.6	3.48	21000	486	1264	1.01	1.08	1.08	1.10
G6-T1	Basler [35]	127	1.5	259.2	4.9	4.04	21000	253	516	1.02	1.10	1.10	1.11
H1T2	Cooper [29]	127	1.5	127.3	9.98	2.48	21000	745	3421	1.07	1.11	1.11	1.12
CP1/1	Narayanan R. [32]	500	1.4	245.1	2.04	3.92	21000	246	88	1.06	1.13	1.13	1.14
G8-T2	Basler [35]	127	1.5	250	5.08	3.76	21000	263	445	0.81	0.87	0.87	0.88
G8-T3	Basler [35]	127	1.5	250	5.08	3.76	21000	263	516	0.94	1.00	1.00	1.02
LS3-	Evans H. R [31]	608	1.5	247.2	2.46	4.11	19700	201	103	1.05	1.07	1.07	1.10
Mean										0.99	1.04	1.04	1.05
S-2	Sakai F. [28]	319	1.8	99.7	3.2	3.28	21000	352	161	1.00	1.02	0.85	0.92
US2/5	Kamtekar.A.G.	359	2.1	113.3	3.17	3.79	21000	230	135	1.12	1.15	0.94	1.02
STG1	Rockey K. C. [26]	279	1.9	139.5	2	3.95	21000	255	60	1.12	1.06	0.94	0.97
STG2	Rockey K. C. [26]	253	1.9	158.1	1.6	4.00	21000	272	40	1.09	1.00	0.93	0.98
G7	Lee [9]	600	2	150	4	2.50	20500	285.2	258.	1.11	1.03	0.96	1.01
G8	Lee [9]	600	2	150	4	4.00	20500	285.2	276.	1.20	1.10	1.02	1.08
2.2	Bergfelt [33]	600	2.4	300	2	3.00	21000	255	75	1.08	0.88	0.88	1.10
Mean										1.10	1.03	0.93	1.01
G8-T1	Basler [35]	127	3	250	5.08	3.76	21000	263	375	1.07	0.75	0.75	1.02
H1-T2	Nishino [36]	127	3	127	9.98	2.48	21000	745	2803	1.34	0.94	0.94	1.20
G1-1	Nishino [36]	120	3	182	6.6	3.48	20500	486.3	970.	1.22	0.86	0.86	1.16
G2-1	Nishino [36]	950	3	144	6.6	2.88	20500	486.3	960.	1.35	0.96	0.96	1.20
Mean										1.25	0.88	0.88	1.15
C-AC2	Carskaddan P.S.	457	5.4	147.5	3.1	3.13	21000	215	120	1.46	1.01	0.90	1.05
C-AC4	Carskaddan P.S.	457	5.5	106.3	4.3	3.79	21000	236	245	1.31	1.17	0.96	1.09
C-AC5	Carskaddan P.S.	457	5.5	106.3	4.3	4.44	21000	236	232	1.24	1.11	0.91	1.03
Mean										1.34	1.10	0.92	1.06